

Constraints of the equation of state of dark energy from current and future observational data by piecewise parametrizations

Qiping Su^{1,*} Xi He^{1,†} and Rong-Gen Cai^{2‡}

¹ *Department of Physics, Hangzhou Normal University, Hangzhou, 310036, China*

² *State Key Laboratory of Theoretical Physics,
Institute of Theoretical Physics, Chinese Academy of Sciences,
Post Office Box 2735, Beijing 100190, China*

(Dated: June 15, 2021)

Abstract

The model-independent piecewise parametrizations (0-spline, linear-spline and cubic-spline) are used to estimate constraints of equation of state of dark energy (w_{de}) from current observational data (including SNIa, BAO and Hubble parameter) and the simulated future data. A combination of fitting results of w_{de} from these three spline methods reveal essential properties of real equation of state w_{de} . It is shown that w_{de} beyond redshift $z \sim 0.5$ is poorly constrained from current data, and the mock future ~ 2300 supernovae data give poor constraints of w_{de} beyond $z \sim 1$. The fitting results also indicate that there might exist a rapid transition of w_{de} around $z \sim 0.5$. The difference between three spline methods in reconstructing and constraining w_{de} has also been discussed.

* sqp@hznu.edu.cn

† hexi@hznu.edu.cn

‡ cairg@itp.ac.cn

I. INTRODUCTION

The current expansion of the universe is found to be accelerating [1, 2], one of the possible explanations for this is the existence of dark energy(DE), whose energy density is dominant in the universe and its present equation of state w_{de0} is less than $-1/3$. At present, it is still fair to say that one knows a little about the nature of DE. From current astronomical observational data, we can obtain some properties of the equation of state w_{de} (the ratio of the pressure and energy density of DE). To fit the observational data, one has to first assume a form of w_{de} . Some forms of w_{de} have been used in the literature. For example, the CPL parametrization $w_{de}(z) = w_0 + w_a z/(1+z)$ [3, 4] and the redshift expansion, $w_{de}(z) = w_0 + w_z z$ [5–8]. It has been found that w_{de} is very close to -1 and should be varying very slowly with redshift (if any). In the most cases, the cosmological constant with $w = -1$ is still favored within 2σ confidence level (C.L.). Of course the fitting results are dependent on the parametrization forms adopted. Usually a parametrization form is only suitable to mimic one type of $w_{de}(z)$. For example, the CPL parametrization can describe linear and smooth w_{de} well but is hard to reconstruct w_{de} with oscillations or rapid transitions. On the other hand, several model-independent methods have also been proposed to reconstruct $w_{de}(z)$ [9–13], e.g., the uncorrelated band-power estimate (i.e., 0-spline) [14], cubic-spline method [15], linear-spline method [16–18], wavelet approach [19], and Gaussian process modeling [20–22], etc. Most of model-independent methods have a piecewise $w_{de}(z)$:

$$w_{de}(z) = w_i(z), \quad z_i < z \leq z_{i+1}, \quad (1)$$

where $w_i(z)$ is a simple function of redshift z , e.g., $w_i(z)$ is just a constant in each bin for the 0-spline method.

Different model-independent methods should give different but consistent fitting results of DE. In this paper, we would like to get constraints of w_{de} from present and next generational observations by using three piecewise parametrizations: 0-spline, linear-spline and cubic-spline. The difference among the three spline methods in constraining w_{de} will be analyzed. It is shown that each spline method is only suited to certain types of w_{de} . A combination of constraints of w_{de} from the three spline methods should help to get real properties of w_{de} .

At first, the constraints of w_{de} from current observational data will be obtained. It is found that the present constraints on w_{de} are very weak beyond $z \sim 0.5$, because in the higher redshift region there are less data points and the effect of DE on the expansion of the

universe is weaker. Moreover, we see from the fitting results from 0-spline and linear-spline methods that there might exist a rapid transition of w_{de} around $z = 0.5$. To estimate the constraints on w_{de} from next generation observations, ~ 2300 SN data as forecasted for a space mission like SNAP/JDEM [23, 24] are simulated. The mock data are simulated from two fiducial models: one with a smooth w_{de} and the other with a rapid transition w_{de} around $z = 0.5$. In this case w_{de} is poorly constrained after $z \sim 1$.

II. THE CONSTRAINTS ON w_{de} FROM PRESENT DATA

We use three spline methods to get constraints of w_{de} from present observational data, which include type Ia supernovae data (SNIa), baryon acoustic oscillation (BAO) and observational Hubble data. The best-fitting parameters and their errors will be obtained by using the Markov Chain Monte Carlo (MCMC) method. In general, the errors of w_{de} of different bins are correlated. We will adopt the decorrelated method proposed in [10] to obtain errors of a new parameter $Q(z)$. The new parameter $Q(z)$ is defined by transforming the covariance matrix of w_{de} , so that the errors of $Q(z)$ are uncorrelated and do not entangle in each bin.

A. Observational data

Since it is hard to get strong constraints of w_{de} in high redshift region, we will focus on constraining w_{de} in the region $z \in [0, 0.9]$ only in this work. The data sets we adopt are SNIa Union2 data [25], BAO distance parameter A [26] and observational Hubble data from [28–30]. Those data points with $z > 0.9$ in these data sets will be abandoned. As a result, in our calculations, only 519 SNIa data points, 11 Hubble data points and one BAO data point are used. In this case, one needs not to assume the form of $w_{de}(z > 0.9)$ and to consider correlations between $w_{de}(z > 0.9)$ and $w_{de}(0 \leq z \leq 0.9)$.

The cosmological parameters are fitted with the SNIa data [31] by

$$\chi_{SN}^2 = \sum_{i=1}^{519} \frac{[\mu_{th}(z_i) - \mu_{ob}^i]^2}{\sigma_i^2}, \quad (2)$$

where the theoretical distance modulus

$$\mu_{th}(z) = 5 \log_{10} D_L + \mu_0. \quad (3)$$

For a flat Friedmann-Robertson-Walker universe, the luminosity distance is

$$D_L = (1+z) \int_0^z dx/E(x) , \quad (4)$$

where

$$E^2(z) = \Omega_{m0}(1+z)^3 + (1-\Omega_{m0})F(z). \quad (5)$$

Here Ω_{m0} is the current fractional matter density of the universe and function $F(z)$ depends on the parametrization of $w_{de}(z)$:

$$F(z) = e^{3 \int_0^z \frac{1+w_{de}}{1+x} dx}. \quad (6)$$

One can expand Eq.(2) with respect to μ_0 as

$$\chi_{SN}^2 = a + 2b\mu_0 + c\mu_0^2 \quad (7)$$

where

$$\begin{aligned} a &= \sum_{i=1}^{519} \frac{[\mu_{th}(z_i; \mu_0 = 0) - \mu_{ob}^i]^2}{\sigma_i^2}, \\ b &= \sum_{i=1}^{519} \frac{\mu_{th}(z_i; \mu_0 = 0) - \mu_{ob}^i}{\sigma_i^2}, \\ c &= \sum_{i=1}^{519} \frac{1}{\sigma_i^2}. \end{aligned} \quad (8)$$

The χ_{SN}^2 has a minimum with respect to μ_0 ,

$$\tilde{\chi}_{SN}^2 = a - b^2/c. \quad (9)$$

This way the nuisance parameter μ_0 is reduced, in this work we will adopt $\tilde{\chi}_{SN}^2$ instead of χ_{SN}^2 .

The BAO distance parameter A is the measurement of BAO peak in the distribution of SDSS luminous red galaxies [26]

$$A = \Omega_{m0}^{1/2} E^{-1/3}(0.35) \left(\frac{1}{0.35} \int_0^{0.35} \frac{dz}{E(z)} \right)^{2/3}. \quad (10)$$

The value of A is determined to be $0.469(n_s/0.98)^{-0.35} \pm 0.017$, where $n_s = 0.963$ is the scalar spectral index, which has been updated from the WMAP7 data [27]. The χ_A^2 is defined as

$$\chi_A^2 = \frac{(A - 0.472)^2}{0.017^2}. \quad (11)$$

z	0	0.1	0.17	0.27	0.4	0.48	0.88	0.9	0.24	0.34	0.43
h	0.738	0.69	0.83	0.77	0.95	0.97	0.9	1.17	0.7969	0.838	0.8645
σ_h	0.024	0.12	0.08	0.14	0.17	0.6	0.4	0.23	0.0232	0.0296	0.0327

TABLE I. 11 observational Hubble data with their redshifts from [28–30].

The observational Hubble data can be obtained by using the differential ages of passively evolving galaxies

$$H \simeq -\frac{1}{1+z} \frac{\Delta z}{\Delta t}. \quad (12)$$

Here we adopt 11 observational Hubble data points with $z \leq 0.9$ from [28–30]. Those data points are summarized in Table I. The χ_{HUB}^2 is defined as:

$$\chi_{HUB}^2 = \sum_{i=1}^{11} \frac{[h_{th}(z_i) - h_{ob}(z_i)]^2}{\sigma_{h,i}^2}, \quad (13)$$

where $h = H/100 \text{ km} \cdot \text{s}^{-1} \cdot \text{Mpc}^{-1}$.

Finally the total χ_T^2 for three kinds of observational data is the sum of them:

$$\chi_T^2 = \tilde{\chi}_{SN}^2 + \chi_A^2 + \chi_{HUB}^2. \quad (14)$$

B. Methodology and Results

Now by the piecewise parametrization approaches for w_{de} , we get the constraints of w_{de} from the observational data mentioned in the above. We will use the 0-spline, liner spline and cubic spline method, respectively. The best-fitting $w_{de}(z)$, $Q(z)$ and their 1σ , 2σ C.L. errors obtained by using three spline methods are plotted in Fig. 1. One can see that the constraints of w_{de} from the three methods are consistent with each other. It is shown that the constraints of w_{de} beyond $z \sim 0.5$ are much weaker than those within $z \sim 0.5$, and $w_{de} = -1$ (the cosmological constant) is still consistent with present constraints of w_{de} at 2σ C.L. In addition, there might exist a rapid transition of w_{de} around $z = 0.5$, which is particularly evident in the fitting results from the 0-spline and linear-spline methods.

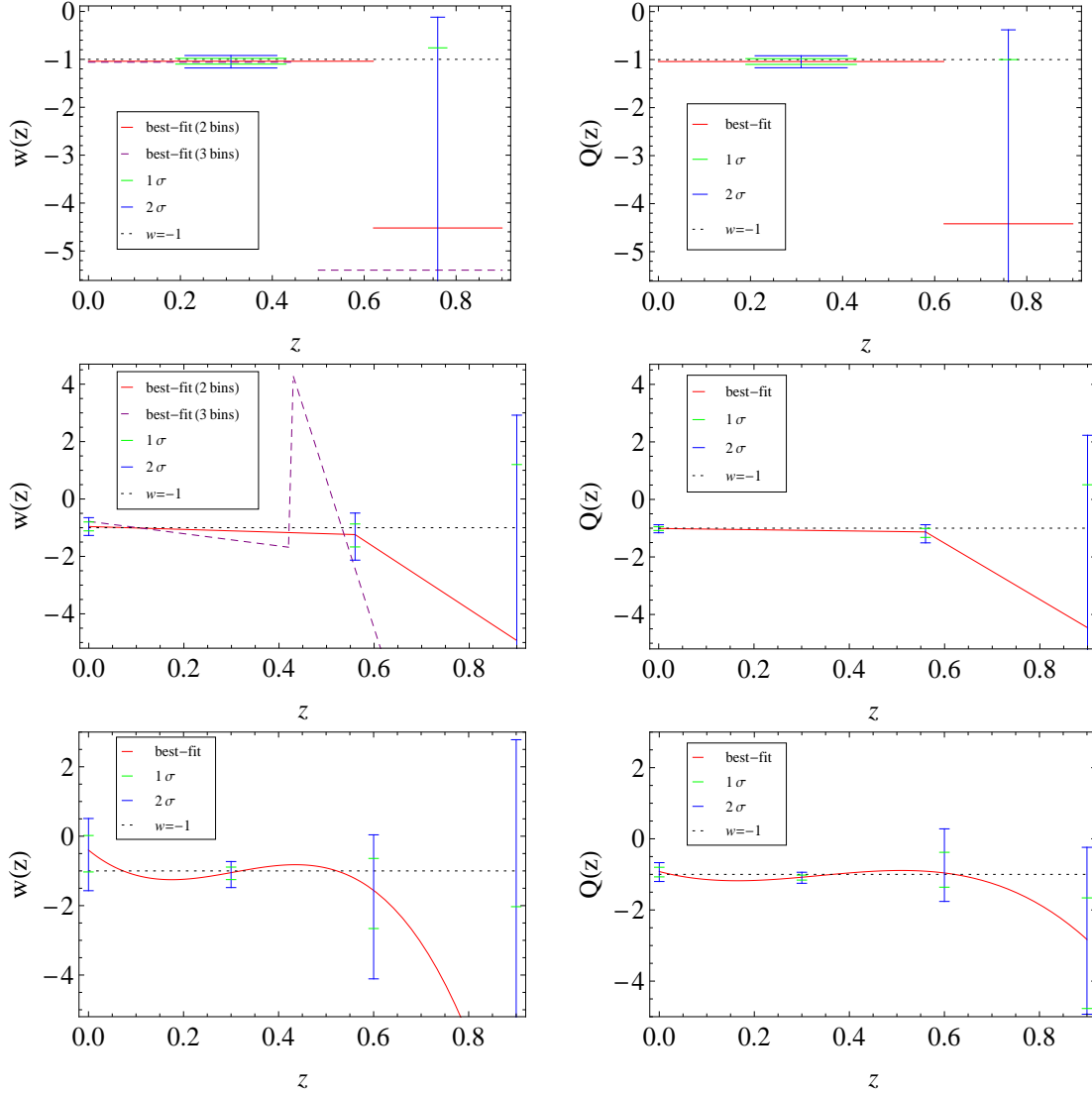


FIG. 1. The best fitting $w_{de}(z)$, $Q(z)$ and their 1σ and 2σ C.L. errors from the current observational data (SN+A+HUB). The black dotted curves stand for $w = -1$. The three figures in left panel are for the correlated $w_{de}(z)$ and the three figures in right panel are for the uncorrelated parameters $Q(z)$. The upper two figures are from the 0-spline method, the middle two from the linear-spline method and the bottom two from the cubic-spline method. Note that some best fitting results on w_{de} and their errors are not included in figures when they are beyond the range of figures.

1. 0-spline method

In this method, one divides the redshift region under consideration into n bins, and sets

$$w_{de}(z_i < z \leq z_{i+1}) = w_i , \quad (15)$$

where w_i are constants and z_i are divided positions of bins. Since the number and precision of present data are still not sufficient enough, at first we divide the redshift region $[0, 0.9]$ into only two bins and treat the divided position z_1 as a free parameter of the model. By fitting the model with data, we find the best value of divided position $z_1 = 0.62$. Thus we have

$$w_{de}(z) = \begin{cases} w_1 , & 0 \leq z \leq 0.62 \\ w_2 , & 0.62 < z \leq 0.9 \end{cases} . \quad (16)$$

In the fitting process we have assumed a prior $-20 < w_2$. Otherwise w_2 would go to a very large minus value in MCMC procedure and thus the downward error of w_2 would be extremely large. Of course the prior will not qualitatively affect the results and conclusions of this paper. It is found that there is almost no difference between the errors of w_i and corresponding Q_i . This shows that the correlation between w_1 and w_2 is extremely small in this case.

The fitting results are shown in Table II and Fig. 1. It indicates that the constraints of w_{de} are very good in the whole first bin, since here we have assumed w_{de} to be a constant and the errors of w_{de} are averaged in each bin. For the second bin, the errors of w_2 are very large, particularly its downward error, as expected. Of course the fitting results depend on the number of bins and the divided manners. Here the width of the second bin is relatively small and there are only 103 data points in this bin, but the main reason for the weak constraint of w_2 (w_{de} in the second bin) is due to the high redshift; in the lower redshift region, the same width of bin and the same number of data points can give much better constraints of w_{de} .

Next we divide the redshift region $z \in [0, 0.9]$ into three bins to see whether there exist more structures of $w_{de}(z)$ in this region. Two divided positions are also treated as free parameters, the positions of them from the best fitting are: $z_1 = 0.45$ and $z_2 = 0.50$. In this

h	Ω_{m0}	w_1 and Q_1	w_2 and Q_2	χ^2_{min}
$0.722^{+0.012+0.025}_{-0.014-0.028}$	$0.275^{+0.022+0.042}_{-0.015-0.033}$	$-1.04^{+0.06+0.12}_{-0.06-0.14}$	$-4.52^{+3.76+4.40}_{-15.38-15.47}$	499.832
		$-1.04^{+0.06+0.12}_{-0.06-0.13}$	$-4.42^{+3.42+4.04}_{-15.00-15.05}$	

TABLE II. The best-fitting values with 1σ and 2σ C.L. errors of parameters from present data in the case with the 0-spline method.

case, the second bin is relatively narrow. The best-fitting $w_{de}(z)$ is found to be:

$$w_{de}(z) = \begin{cases} -1.06, & 0 \leq z \leq 0.45 \\ 5.82, & 0.45 < z \leq 0.5 \\ -5.40, & 0.5 < z \leq 0.9 \end{cases} . \quad (17)$$

This results are plotted in Fig. 1, but the result for the second bin $w_2=5.82$ is not included because it deviates far from w_{de} in other bins. The appearance of the narrow second bin and the large deviation of w_2 from the values in other bins might imply that there is a rapid transition of w_{de} around $z \sim 0.5$. Mock future data with a rapid transition w_{de} around $z \sim 0.5$ is simulated in the next section and a similar fitting result from the data is found.

2. Linear-spline method

In this case we set $w_{de}(z)$ as

$$w_{de}(z_{i-1} < z \leq z_i) = w(z_{i-1}) + \frac{w(z_i) - w(z_{i-1})}{z_i - z_{i-1}}(z - z_{i-1}), \quad (1 \leq i \leq n) \quad (18)$$

where n is the number of bins and $z_0 = 0$. Still, the redshift region $z \in [0, 0.9]$ is divided into two bins and the best fitting result gives the divided position to be $z_1 = 0.56$, which is very close to the one given by 0-spline method. Here the prior $-20 \leq w(0.9)$ has been assumed. The best fitting values of the parameters $w(0)$, $w(0.56)$ and $w(0.9)$ and their errors are shown in Fig. 1 and Table III. It is shown that the errors of w_{de} in the second bin (especially the downward error) increase quickly with redshift z . At $z = 0.9$, the constraint of w_{de} becomes extremely weak.

The best-fitting $w_{de}(z)$ in $[0, 0.9]$ with three bins is also shown in Fig. 1. The best fitting results for w_{de} are: $w(0) = -0.78$, $w(0.42) = -1.68$, $w(0.43) = 4.28$ and $w(0.9) = -20$. Note that here we have also assumed the prior $-20 \leq w(0.9)$. One can see from the figure

that there is also a rapid transition of w_{de} around $z \sim 0.5$ in this best fitting, as the case of the 0-spline method.

h	Ω_{m0}	$w(0)$ and $Q(0)$	$w(0.56)$ and $Q(0.56)$	$w(0.9)$ and $Q(0.9)$	χ^2_{min}
$0.721^{+0.012+0.026}_{-0.013-0.027}$	$0.276^{+0.026+0.046}_{-0.015-0.035}$	$-0.96^{+0.16+0.31}_{-0.15-0.31}$ $-1.01^{+0.06+0.13}_{-0.07-0.15}$	$-1.24^{+0.37+0.75}_{-0.43-0.89}$ $-1.13^{+0.12+0.25}_{-0.19-0.38}$	$-4.93^{+6.13+7.85}_{-15.06-15.06}$ $-4.46^{+4.97+6.69}_{-13.02-13.08}$	499.692

TABLE III. The best-fitting values with 1σ and 2σ C.L. errors of parameters from present data in the case with the linear-spline method.

3. Cubic-spline method

To use the cubic-spline method, we divide $z \in [0, 0.9]$ into three bins with the fixed divided positions as: $z_1 = 0.3$, $z_2 = 0.6$. The results are shown in Fig. 1 and Table IV. In this case, once again, the constraints of w_{de} in the last bin are very weak and the errors of w_{de} are extremely large. The errors of the uncorrelated parameter $Q(0.9)$ are much smaller than those in other two methods but the errors of other Q 's are larger than those in other two methods, because in the cubic-spline method w_{de} in different bins are highly correlated.

h	Ω_{m0}	$w(0)$ and $Q(0)$	$w(0.3)$ and $Q(0.3)$	$w(0.6)$ and $Q(0.6)$	$w(0.9)$ and $Q(0.9)$	χ^2_{min}
$0.720^{+0.013+0.026}_{-0.013-0.027}$	$0.278^{+0.026+0.049}_{-0.015-0.035}$	$-0.40^{+0.42+0.91}_{-0.63-1.17}$ $-0.92^{+0.12+0.25}_{-0.15-0.28}$	$-1.05^{+0.16+0.32}_{-0.20-0.43}$ $-1.08^{+0.06+0.14}_{-0.08-0.17}$	$-1.56^{+0.92+1.60}_{-1.10-2.55}$ $-0.96^{+0.58+1.24}_{-0.40-0.80}$	$-9.88^{+7.85+12.66}_{-10.09-10.11}$ $-2.83^{+1.17+2.59}_{-1.94-2.10}$	498.942

TABLE IV. The best-fitting values with 1σ and 2σ errors of parameters from present data in the case with the cubic-spline method.

III. CONSTRAINTS OF w_{de} FROM FUTURE DATA

To see the constraint ability on w_{de} from future observational data, we adopt the characteristics of a SNAP-like JDEM survey [23] to simulate the future SN data with $0.1 < z < 1.7$, which include 1998 SN data points. The redshift distribution of the mock SN data is shown

$z \rightarrow$	0.1	0.2	0.3	0.4	0.5	0.6	0.7	0.8	0.9	1.0	1.1	1.2	1.3	1.4	1.5	1.6	1.7
N_{bin}	300	35	64	95	124	150	171	183	179	170	155	142	130	119	107	94	80

TABLE V. The redshift distribution of 1998 SN data with $0.1 < z < 1.7$ for a SNAP-like JDEM survey [23] and 300 SN data with $z < 0.1$ from the NSNF [24]. The redshifts in the first row are the upper limits of each bin.

in Table V, in which 300 supernovae with $z < 0.1$ [19, 24] are also included. In each redshift bin as shown in Table V, SN's are assumed to be uniformly distributed.

We will use two fiducial models to simulate the mock data:

Model I: one assumes a slowly varying equation of state for DE:

$$w_{de}(z) = -0.8 - \frac{300000}{e^{22/(1+z)} + 600000} ; \quad (19)$$

Model II: one has the equation of state with a rapid transition around $z \sim 0.5$:

$$w_{de}(z) = -0.8 - \frac{3 \times 10^{14}}{e^{100/(1+z)-30} + 6 \times 10^{14}} ; \quad (20)$$

In Fig. 2 two fiducial $w_{de}(z)$ are plotted. The form of $w_{de}(z)$ in these two models is also adopted in [20]. Both fiducial models have $h = 0.72$ and $\Omega_{m0} = 0.28$. Now the distance modulus of ~ 2300 SN can be simulated and the corresponding errors are assumed as [19, 23]:

$$\sigma(z) = \sqrt{\frac{\sigma_{obs}^2}{N_{bin}} + dm^2}, \quad (21)$$

where $\sigma_{obs} = 0.15$, $dm = 0.02z/z_{max}$ and z_{max} is the maximum redshift (here $z_{max} = 1.7$). To simulate the effect of other future observations and alleviate the degeneracy between Ω_{m0} and w_{de} , we add a prior $\Omega_{m0} = 0.28 \pm 0.03$. In all three spline methods, the redshift region $(0, 1.7)$ will be divided into three bins. Two divided positions are still treated as free parameters in the cases of 0-spline and linear-spline methods, while the divided positions of bins are fixed by hand in the case of cubic-spline method. All fitting results are shown in Fig. 2. One can see that three spline methods give consistent results and the future mock data give poor constraints of w_{de} beyond $z \sim 1$.

A. 0-spline method

For the fiducial model I, the region $(0, 1.7)$ is divided into three relatively uniform bins in the best fitting model, with the divided positions: $z_1 = 0.55$ and $z_2 = 1.27$. The errors of

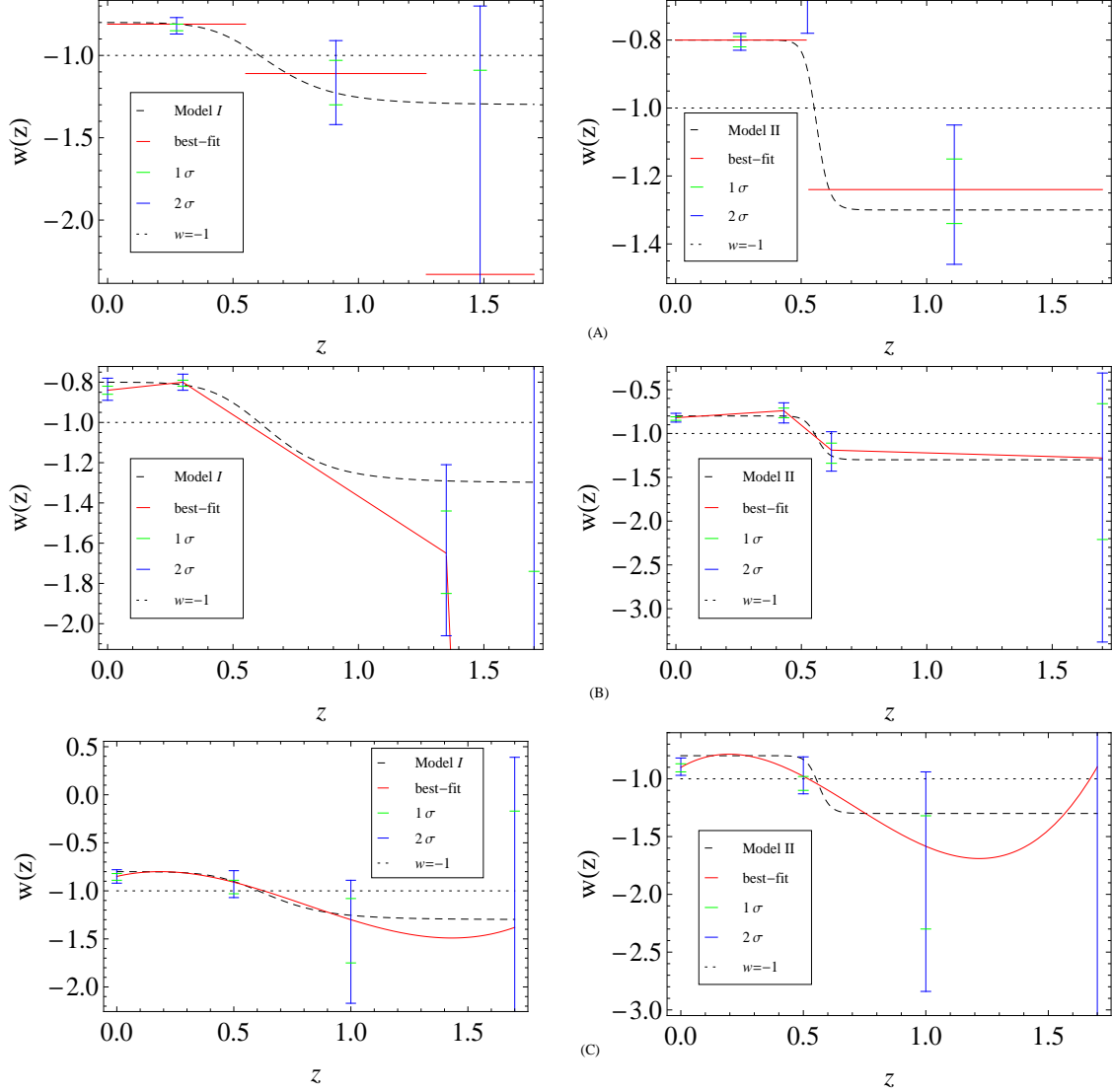


FIG. 2. The best fitting $w_{de}(z)$ and their 1σ and 2σ C.L. errors from the mock future data. The dashed curves are for the fiducial models, and the black dotted curves stand for the cosmological constant $w = -1$. The three figures in left panel are for model I and the three figures in right panel for model II. The upper two figures are from the 0-spline method, the middle ones from the linear-spline method and the bottom two figures from the cubic-spline method.

w_{de} increase rapidly with redshift. In the last bin, the best-fitting w_{de} deviates far from the fiducial model and the errors of w_{de} are relatively large.

For the rapid transition model II, the best fitting divided positions are $z_1 = 0.52$ and $z_2 = 0.53$. In this case the second bin is extremely narrow because of the rapid transition of

the fiducial w_{de} around $z \sim 0.5$. The best fitting w_{de} in the second bin is $w_2 = 0.67$ which deviates from the fiducial w_{de} beyond 2σ C.L. . The errors of w_{de} in the last bin are much better than those for model I, since here the width of last bin is much larger than that in model I.

B. Linear-spline method

In this case the situation is very similar to the case of the 0-spline method. For model I, the best fitting divided positions of bins are $z_1 = 0.3$ and $z_2 = 1.35$. It is shown that the fiducial w_{de} can be well reconstructed until $z \gtrsim 1$. For model II, the best fitting divided positions are $z_1 = 0.43$ and $z_2 = 0.62$. Here the constraints of w_{de} at high redshift are much better than those for model I, since the last bin here is much larger than that for model I. It can be seen that the rapid transition of w_{de} in model II can be well reconstructed by the linear-spline method, as shown in Fig. 2, though the width of second bin is very narrow. The reconstructed w_{de} and its errors here have finer structures than those in the 0-spline method.

C. Cubic-spline method

In this case we fix the divided positions of three bins as $z_1 = 0.5$ and $z_2 = 1.0$. The errors of w_{de} still increase rapidly with redshift. The fitting results for model I and model II indicate that this method can reconstruct the slowly varying w_{de} well, but it is not good in reconstructing the equation of state with rapid transition. For model I the errors of w_{de} are consistent with those from other two methods, but for model II the errors are much larger than those from other two spline methods.

D. Result analysis

For model I, it is shown that w_{de} can be well reconstructed up to $z \sim 1$. For model II, since the width of the last bin are always much larger than that in model I, the errors of w_{de} in the region beyond $z \sim 1$ are much smaller than those in model I (except for the case of the cubic-spline method, which is not good at describing a rapid transition w_{de}). This

means that the fitting results depend on the divided manner of redshift bins. In our case, we treat the divided positions as free parameters and then fix their values to the best-fitting values (in 0-spline and linear-spline methods) or just divide the redshift region uniformly (in the cubic-spline method). In this case, the width of the last bin is always not large enough to get strong constraints of w_{de} in that bin. One may use other ways to divide redshift, even setting the last bin large enough by hand. But a large bin usually will lead to a lose of fine structure of w_{de} in this case.

In the case of the 0-spline method, w_{de} and its errors are averaged in each bin, while in the cases with other two spline methods, the errors of w_{de} increase with redshift inside each bin and the reconstructed w_{de} always have finer structures than that from the 0-spline method. For the cubic-spline method it is good at reconstructing the slowly varying w_{de} , but not the case with rapid transitions, and the errors of w_{de} are highly correlated.

IV. CONCLUSIONS

We have studied the constraint ability on the equation of state w_{de} of dark energy from the present and simulated future observational data by piecewise parametrization with the 0-spline, linear-spline and cubic-spline methods, respectively. Three spline methods give consistent results of w_{de} : 1) the cosmological constant $w_{de} = -1$ is still consistent with present data at 2σ C.L.; 2) current data can constrain w_{de} well up to $z \sim 0.5$ and the future (mock ~ 2300 SN) data can constrain w_{de} well up to $z \sim 1$; 3) in high redshift region, the downward errors of w_{de} are always much larger than the upper ones; 4) the fitting results from current data by using the 0-spline and linear-spline methods indicate that there might exist a rapid transition of w_{de} around $z \sim 0.5$.

There are also differences among the fitting results from the three spline methods. With the 0-spline method w_{de} and its errors get averaged in each bin, and thus it always gives poor structure of w_{de} . Therefore this method is suited to be used to confirm whether w_{de} is a constant (including -1) or not. The linear-spline and cubic-spline methods give finer structure of w_{de} than the 0-spline method. The linear-spline method can reconstruct almost all types of w_{de} in principle, but the reconstructed w_{de} is always not smooth at the divided positions of bins, which will lead to deviations of w_{de} from the real w_{de} around the divided positions. Thus the linear-spline method is suited to reconstruct non-smooth $w_{de}(z)$, and the

positions where w_{de} suddenly changes can be accurately determined. For the cubic-spline method, one needs not to search for the best-fitting divided positions of bins but the redshift region must be divided into at least 3 bins. It is shown that the cubic-spline method is not good at reconstructing w_{de} with rapid transitions and the errors of w_{de} at different bins are highly correlated. The cubic-spline method is therefore suited to reconstruct a smoothly varying w_{de} . Basically, a combination of the fitting results from the three spline methods can reveal the real w_{de} .

The fitting results are also affected by divided manners of redshift bin. Usually a larger width of one bin will lead to a stronger constraint of w_{de} there, but fine structure of w_{de} will be lost. At present, the number and precision of observational data are still not sufficient to obtain both strong constraints and fine structures of w_{de} . In particular, to constrain w_{de} at high redshift, a large number of data will be required [32].

Acknowledgements: This work was supported in part by the National Natural Science Foundation of China (No.10821504, No.10975168, No.11035008, No.11147186 and No.11047001), and the Ministry of Science and Technology of China under grant No. 2010CB833004, and a grant from the Chinese Academy of Sciences and a grant from Hanzhou Normal University.

-
- [1] A. G. Riess *et al.* [Supernova Search Team Collaboration], *Astron. J.* **116**, 1009 (1998) [arXiv:astro-ph/9805201].
 - [2] S. Perlmutter *et al.* [Supernova Cosmology Project Collaboration], *Astrophys. J.* **517**, 565 (1999) [arXiv:astro-ph/9812133].
 - [3] M. Chevallier and D. Polarski, *Int. J. Mod. Phys. D* **10**, 213 (2001) [arXiv:gr-qc/0009008].
 - [4] E. V. Linder, *Phys. Rev. Lett.* **90**, 091301 (2003) [arXiv:astro-ph/0208512].
 - [5] D. Huterer and M. S. Turner, *Phys. Rev. D* **64**, 123527 (2001) [arXiv:astro-ph/0012510].
 - [6] A. R. Cooray and D. Huterer, *Astrophys. J.* **513**, L95 (1999) [arXiv:astro-ph/9901097].
 - [7] D. Huterer and M. S. Turner, *Phys. Rev. D* **60**, 081301 (1999) [arXiv:astro-ph/9808133].
 - [8] J. Weller and A. J. Albrecht, *Phys. Rev. Lett.* **86**, 1939 (2001) [arXiv:astro-ph/0008314].
 - [9] D. Huterer and G. Starkman, *Phys. Rev. Lett.* **90**, 031301 (2003) [arXiv:astro-ph/0207517].
 - [10] D. Huterer and A. Cooray, *Phys. Rev. D* **71**, 023506 (2005) [arXiv:astro-ph/0404062].

- [11] R. -G. Cai and Q. Su, Phys. Rev. D **81**, 103514 (2010) [arXiv:0912.1943 [astro-ph.CO]].
- [12] Y. Wang, Phys. Rev. D **80**, 123525 (2009) [arXiv:0910.2492 [astro-ph.CO]].
- [13] Y. Wang and M. Tegmark, Phys. Rev. D **71**, 103513 (2005) [astro-ph/0501351].
- [14] S. Sullivan, A. Cooray and D. E. Holz, JCAP **0709**, 004 (2007) [arXiv:0706.3730 [astro-ph]].
- [15] P. Serra, A. Cooray, D. E. Holz, A. Melchiorri, S. Pandolfi and D. Sarkar, Phys. Rev. D **80**, 121302 (2009) [arXiv:0908.3186 [astro-ph.CO]].
- [16] R. G. Cai, Q. Su and H. B. Zhang, JCAP **1004**, 012 (2010) [arXiv:1001.2207 [astro-ph.CO]].
- [17] G. B. Zhao, D. Huterer and X. Zhang, Phys. Rev. D **77**, 121302 (2008) [arXiv:0712.2277 [astro-ph]].
- [18] P. Serra, A. Cooray, D. E. Holz, A. Melchiorri, S. Pandolfi and D. Sarkar, Phys. Rev. D **80**, 121302 (2009) [arXiv:0908.3186 [astro-ph.CO]].
- [19] A. Hojjati, L. Pogosian and G. B. Zhao, JCAP **1004**, 007 (2010) [arXiv:0912.4843 [astro-ph.CO]].
- [20] T. Holsclaw, U. Alam, B. Sanso, H. Lee, K. Heitmann, S. Habib, D. Higdon, Phys. Rev. Lett. **105**, 241302 (2010) [arXiv:1011.3079 [astro-ph.CO]].
- [21] T. Holsclaw, U. Alam, B. Sanso, H. Lee, K. Heitmann, S. Habib, D. Higdon, Phys. Rev. **D82**, 103502 (2010) [arXiv:1009.5443 [astro-ph.CO]].
- [22] T. Holsclaw, U. Alam, B. Sanso, H. Lee, K. Heitmann, S. Habib, D. Higdon, [arXiv:1104.2041 [astro-ph.CO]].
- [23] A. G. Kim, E. V. Linder, R. Miquel and N. Mostek, Mon. Not. Roy. Astron. Soc. **347**, 909 (2004) [astro-ph/0304509].
- [24] G. Aldering *et al.*, Proc. SPIE, 4836,61 (2002)
- [25] R. Amanullah, C. Lidman, D. Rubin, G. Aldering, P. Astier, K. Barbary, M. S. Burns and A. Conley *et al.*, Astrophys. J. **716**, 712 (2010) [arXiv:1004.1711 [astro-ph.CO]].
- [26] D. J. Eisenstein *et al.* [SDSS Collaboration], Astrophys. J. **633**, 560 (2005) [astro-ph/0501171].
- [27] E. Komatsu *et al.* [WMAP Collaboration], Astrophys. J. Suppl. **192**, 18 (2011) [arXiv:1001.4538 [astro-ph.CO]].
- [28] A. G. Riess, L. Macri, S. Casertano, H. Lampeitl, H. C. Ferguson, A. V. Filippenko, S. W. Jha and W. Li *et al.*, Astrophys. J. **730**, 119 (2011) [Erratum-ibid. **732**, 129 (2011)] [arXiv:1103.2976 [astro-ph.CO]].
- [29] D. Stern, R. Jimenez, L. Verde, M. Kamionkowski and S. A. Stanford, JCAP **1002**, 008 (2010)

- [arXiv:0907.3149 [astro-ph.CO]].
- [30] E. Gaztanaga, A. Cabre and L. Hui, *Mon. Not. Roy. Astron. Soc.* **399**, 1663 (2009) [arXiv:0807.3551 [astro-ph]].
- [31] Q. Su, Z. -L. Tuo and R. -G. Cai, *Phys. Rev. D* **84**, 103519 (2011) [arXiv:1109.2846 [astro-ph.CO]].
- [32] D. H. Weinberg, M. J. Mortonson, D. J. Eisenstein, C. Hirata, A. G. Riess and E. Rozo, arXiv:1201.2434 [astro-ph.CO].